

# A New Approach of Geological Disasters Forecasting using Meteorological Factors based on Genetic Algorithm Optimized BP Neural Network

Sunwen Du<sup>1</sup>, Jin Zhang<sup>1</sup>, Zengbing Deng<sup>2</sup>, Jingtao Li<sup>2</sup>

<sup>1</sup>College of Mining Technology, Taiyuan University of Technology,  
Yingze West St. 79, 030024 Taiyuan, P. R. China

<sup>2</sup>Department of Coal Quality and Geologic Survey, China Coal Pingshuo Group co., Ltd,  
Pingshuo Living Quarters, 036006 Shuozhou, P. R. China  
wendu\_sun@163.com

**Abstract**—The monitoring and forecasting of the mining slope deformation are of great significance to prevent potential geological disasters in mining regions and the geological factors have been widely used for the purpose of mining slope deformation monitoring. However, literature review shows that very little work has been done in prediction of mining slope deformation using meteorological factors. To address this issue, a new method is proposed using the meteorological factors to forecast the mining slope deformation. Herein, the meteorological factors include the temperature, atmospheric pressure, cumulative rainfall, relative humidity and refractive index of the mining slope. A genetic algorithm optimized BP neural network (GA-BPNN) was employed to fuse the meteorological factors to establish the prediction model for the mining slope deformation. The experiments have been implemented to evaluate the new approach and a comparison between the GA-BPNN, BPNN and radial basis function neural network (RBF) prediction models has been carried out. The analysis results show that the proposed method can provide precise prediction of the mining slope deformation and its performance is superior to its rivals.

**Index Terms**—Geologic measurements, meteorological factors, forecasting, artificial neural networks.

## I. INTRODUCTION

The geological disasters such as mining subsidence and mine slope landslide are widespread in the deep loose layers of mining regions in Eastern and Northern China, leading to huge economic loss and catastrophe in the mining production activities [1,] [2]. Thus, the monitoring of the mine slope condition is of great importance to assess the health condition of mining regions and ensure the mining operation safety.

In recent years, the security level of the mining slope is evaluated through forecasting and monitoring the deformation of the mine slope [3]. This has been achieved by utilizing all kinds of related external influencing factors such

as various geological and meteorological data [4]. The geological influencing factors have been widely studied to investigate the mine geological disasters [4], [5]. However, it is always difficult to directly monitor the geological parameters due to the complexity of the mine slope structure. The sensors for geological parameters detection are hardly installed in practice. Alternatively, the meteorological factors can be easily measured in practice. The meteorological factors include the temperature, atmospheric pressure, cumulative rainfall throughout the year, relative humidity and refractive index of the mine slopes, etc. These factors also have important impacts on slope deformation and they can reflect the deformation condition of the mine slopes. Hence, it is possible to monitor the deformation of the mine slopes using the meteorological factors.

However, many researches have been done using the geological factors for the purpose of mining slope deformation monitoring while very limited work has been done using meteorological factors. Among existing predictors when using geological and meteorological data, there are mainly three methodologies, i.e. the grey theory prediction [6], [7], time series prediction [8] and artificial neural network [9]. The grey theory prediction has the optimal and unique ability of performing fitting predictions using small data sets but suffers from prediction accuracy for many actual systems [7]. The accuracy of the mine slope deformation data monitoring could reaches centimeter order in magnitude. So the grey theory prediction method is not suitable for this application. The time series prediction [10] can learn the relationship between the forecast target and the time course. However, the time series prediction may seldom consider the external factors out of the time series while the mine slope deformation is always under the various external influences. Artificial neural network (ANN) [9], [11] has significant advantages in possessing associative inference and adaptive capacity, and particularly it can be applied to processing various kinds of nonlinear problems [10]. ANN has already been proven to have relatively high precision in predicting the surface

Manuscript received April 29, 2013; accepted December 31, 2013.

This research was funded by a grant (No. 2013AA122301) from the National High Technology Research and Development Program of China (863 Program).

subsidence in mining [12]–[16]. The back propagation neural network (BPNN) is the most popular used ANN [17]. However, the gradient descent training algorithm of BPNN has been theoretically and experimentally proven to be ineffective in the network training. The premature phenomenon restricted the applications of the BPNN [18]. Since the GA has strong ability of finding a global minimum [19], it is worth investigating the GA trained BPNN in prediction of the mine slope deformation.

In order to forecast the deformation of mine slopes in a practical manner, this work presents a new approach by the use of meteorological factors. The novelty of the work is that for the first time, the GA optimized BPNN has been introduced to establish the nonlinear mapping relationship between slope deformation and its meteorological influencing factors. Experimental tests have been carried out to evaluate and validate the performance of the proposed method for mine slope deformation forecasting.

## II. DESCRIPTION OF THE PROPOSED APPROACH

### A. Influence Mechanism of the Meteorological Factors

The meteorological factors, such as the temperature and the rainfall, etc., can provide significant evidence to the deformation condition of the mine slopes [19]. On one hand, the surface runoff is the main external force to crush the mine slope. The crush force of the surface runoff may corrode the slope surface, erode the slope toe, and generate the gully network. On the other hand, the rainfall infiltration will increase the pore water pressure and make the cohesive force of the soil and damping force decreased. As a result, the rainfall could induce the slope landslide. Figure 1 shows the mechanism of action of rainfall on slope landslide.

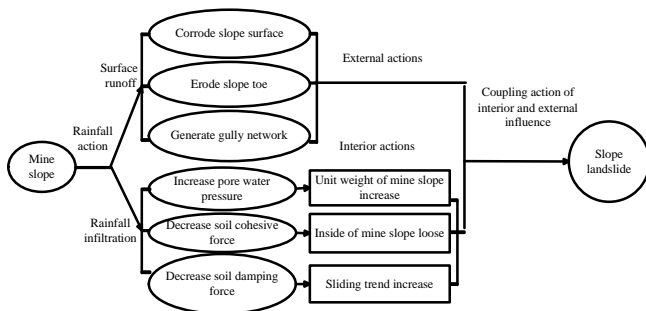


Fig. 1. The mechanism of rainfall action on slope landslide.

TABLE I. THE RELATIONSHIP BETWEEN SLOPE SLIDE SITUATION AND RAINY SEASON IN CHINA DURING MAY TO SEPTEMBER, 1989.

District	Number of landslides	Number of landslides during the rainy season	Percentage (%)
Bijie Guizhou	42	40	96
Wanxian Chongqing	294	256	87
Liangshan Szechwan	212	203	95
Northern region of Szechwan	218	214	98
The river valley in Jinsha river	477	458	96
Longnan region	213	203	95
YiLiang Yunnan	75	71	94
Total	1531	1445	94

It is reported in [19] that the landslide is prone to happen in rainy season. Table I gives the statistic of the occurrence rate of the landslide in rainy seasons in China. It can be seen in the table that the rainfall has significant influence on the landslide.

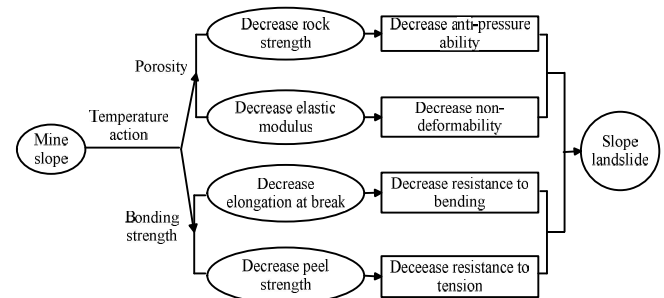


Fig. 2. The mechanism analysis of temperature action on slope landslide.

The temperature may increase the porosity effect of the rock mass and decrease the bonding strength. As a result, the rock strength, elastic modulus, elongation at break, and peel strength are all decreased. Figure 2 shows the mechanism of action of rainfall on slope landslide.

Hence, it can be seen from Fig. 1 and Fig. 2 and Table I that the rainfall and temperature could be used as important indexes to indicate the deformation condition and landslide of the mine slopes. Besides these two indicators, some other meteorological factors also have strong influence or/and connection to the deformation condition of mine slopes, such as the, atmospheric pressure, relative humidity and refractive index [20], [21]. All of them will be adopted to predict the deformation condition of mine slopes in this work.

### B. The GA Optimized BPNN

As discussed in Section I, a new method based on the combination of BPNN and GA is presented to forecast the deformation of mine slope.

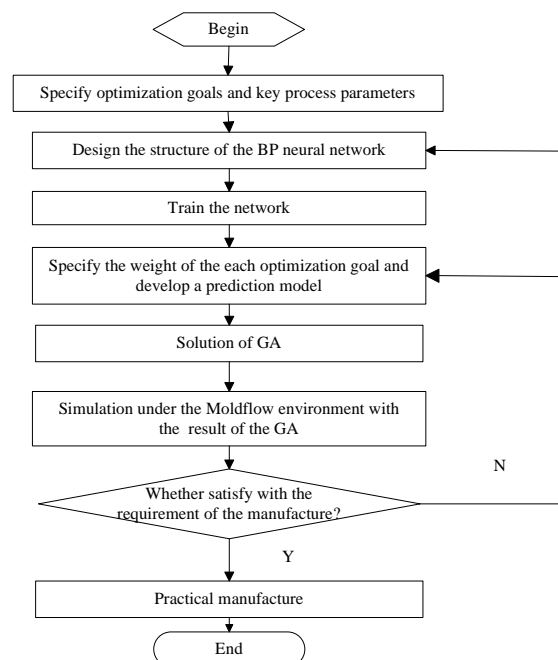


Fig. 3. The flow chart of GA Optimized BPNN method.

The BPNN generally uses the gradient descent method to adjust weight values and threshold values between neurons in

different network layers to make the actual output of the network close to the desired value [16]. However, this gradient descent learning mechanism often suffers from the local minimum. To overcome this shortcoming, the GA is used to quickly search the global optimal value to optimize the BPNN. The detail of the theory of GA can be referred to [19]. In this paper, the link weights and thresholds of the BPNN are optimized by GA. Figure 3 illustrates the solution procedure of the GA optimized BPNN method for deformation forecasting of mine slope.

### C. The Proposed Forecasting Approach

In this work, the meteorological data is used to predict the deformation of the mine slope using the proposed GA-BPNN. The inputs of the BPNN are the temperature, atmospheric pressure, cumulative rainfall, relative humidity and refractive index of the mining slope. Due to the strong randomness of the wind speed and direction, they are not chosen as the input variables. The outputs of the BPNN are east coordinates, north coordinates and elevation coordinates of the monitored positions. Figure 4 shows the forecasting process of the proposed method.

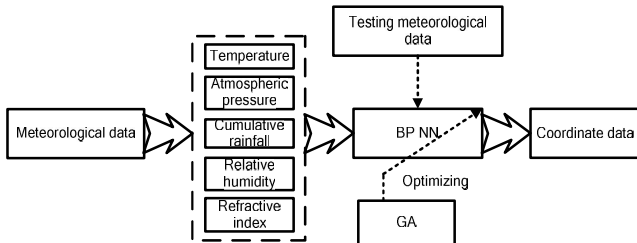


Fig. 4. The diagram of the intelligent forecasting method.

The detailed implementation of GA-BPNN could be described as follows:

- (1) Determine the structure of BPNN,  $5 \times n \times 3$ , where  $n$  is the neural number in hidden layer;
- (2) Set the initial values of the weight coefficients connecting the input layer, hidden layer and output layer of the BPNN;
- (3) Code the chromosomes of the weight coefficients and set the GA parameters (i.e. the replication, crossover and mutation rates);
- (4) Design the fitness function and calculate the corresponding fitness value of current chromosomes;
- (5) Do the crossover and mutation to produce the best fitness values;
- (6) End the optimization if the results can satisfy the termination conditions.

Usually, the fitness function can be designed as

$$fitness = \frac{1}{n} \left| \sum_{i=1}^n (p_i - t_i)^2 \right|, \quad (1)$$

where  $t_i$  is the actual values,  $p_i$  is the BPNN outputs, and  $n$  is the number of samples.

### III. EXPERIMENTAL SETUP

In the experiments, the meteorological factors have been collected using a Slope Stability Radar (SSR). The collected

meteorological factors include the temperature, atmospheric pressure, cumulative rainfall, relative humidity and refractive index of the mining slope. The deformation information of the monitoring points has also been collected, including the east coordinates, north coordinates and elevation coordinates of the monitoring points. Then the recorded data is used to establish a neural network to forecast the deformation data of the mine slope.

Herein the SSR-XT radar was selected, which is a kind of high-precision, remote and real-time slope stability monitoring radar. Figure 5 shows the topography of the experimental strip mine. The monitoring mining area has five mining platform. The SSR-XT was installed at the platform of the southern part of the strip mine and was responsible for monitoring the northern part of the strip mine. The distance between the SSR radar to the monitoring area was 2 km, which was a suitable range for the SSR radar.



Fig. 5. The topography of the monitoring area in the experiments.

The Weather Transmitter (WXT510) is the main actuator in the SSR-XT to collect the meteorological data. Figure 6 shows the WXT510. WXT510 was used to measure the precipitation, atmospheric pressure, temperature and relative humidity. Herein, the precipitation sensor detects the impact of individual raindrops; then the volume of the drops is approximated to be proportional to the impact value of accumulated rainfall.

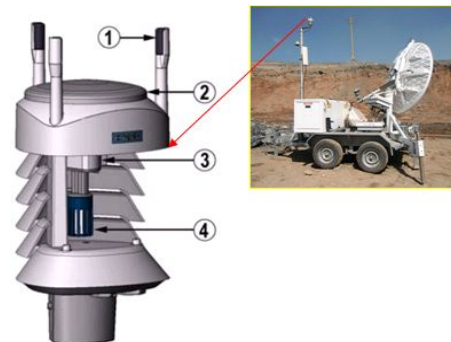


Fig. 6. The cut away view of WXT510: 1 - wind transducers, 2 - precipitation sensor, 3 - pressure sensor, 4 - humidity and temperature sensor.

The diameter of the antenna of the SSR radar reaches to 1.8 meters. This unit could monitor the slope deformation continuously and obtain real-time coordinates deformation data. The collected coordinate data contains east coordinates, north coordinates and elevation coordinates of the monitored positions.

#### IV. APPLICATION OF PROPOSED FORECASTING METHOD

A continuous experiment test of half a year has been carried out from May to November 2012, including the rainy season, to monitor the mine slope of the China Coal Pingshuo group Co., Ltd in North China. In the experiment period a serious landslide happened on 25th July. Hence, we used the meteorological data (i.e. the temperature, atmospheric pressure, cumulative rainfall, relative humidity and refractive index) and the relevant coordinate data from 23th July to 29th July to evaluate the GA-BPNN model. One hundred and fifty samples were recorded. In the analysis, one hundred of the samples were used to train the BPNN and the rest fifty samples were used to test the well-trained BPNN.

In the forecasting process, the BPNN adopted  $5 \times 35 \times 3$  structure. As mentioned above, the GA optimized BPNN approach is proposed for the deformation forecast of the mine slope. The BPNN is capable for simulating the variation tendency of the mine slope deformation and dealing with the nonlinear mapping problem [16]. The GA seeks to improve the generalization ability of the BPNN by optimizing its weight values between the input layer, hidden layer, and output layer. Figure 7 shows the convergence curve and the fitness value of the GA optimization. It can be seen in the figure that in the beginning of the training process, the initial weight values of the BPNN score a low fitness while the GA can search relative

suitable weight values to enhance the prediction ability of the BPNN.

Figure 8 shows the comparison of the prediction for the east coordinate between the radial basis function neural network (RBFNN), BPNN, GA-BPNN. It can be seen in the figure that the prediction precision of the GA-BPNN is higher than that of the RBFNN and BPNN. The prediction error of the GA-BPNN is much smaller than that of the RBFNN and BPNN. This comparison indicates that taking the advantage of the GA optimization, the BPNN could be trained well with high generalization ability and hence the forecasting performance is superior to the unoptimized neural networks.

In order to compare with the classical algorithm, we give the detailed comparison of the BPNN and GA-BPNN. Fig. 9–Fig. 11 show the training performance of the two neural networks. By comparing the mean square error of the training in Fig. 9 it can be seen that BPNN converge to a scheduled accuracy after 9 steps while the GA-BPNN only need 7 steps. Hence the GA can help the BPNN increase the convergence speed. Figure 10 shows the validation results of the trained BPNN. It is noticed from the figure that the gradient index and mutation index of the BPNN is smaller than that of the GA-BPNN. It seems that the trained BPNN is better than the GA-BPNN; however, it is evident in Fig. 9 that the prediction performance of BPNN is lower than the GA-BPNN.

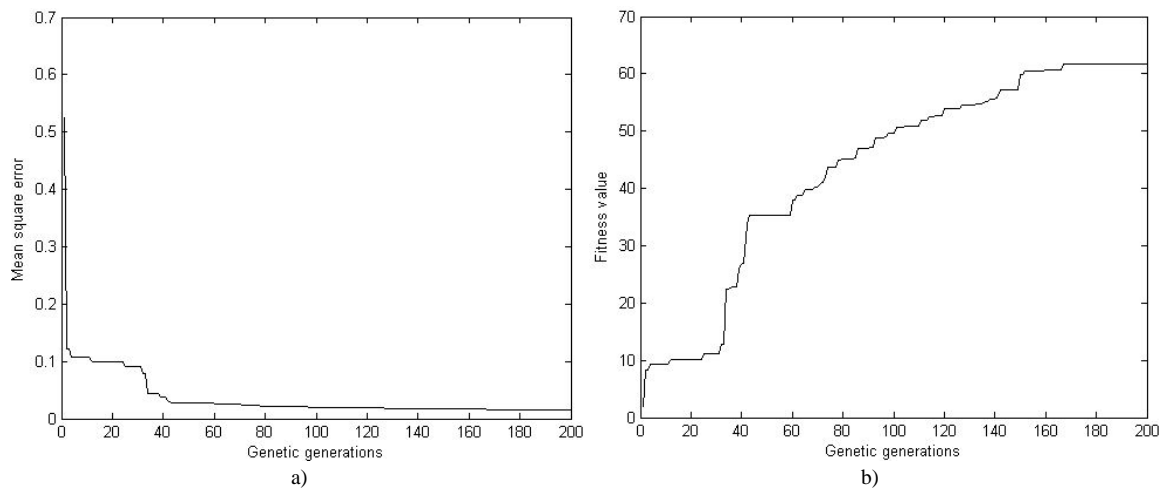


Fig. 7. The GA optimization: (a) convergence curve of the optimization and (b) fitness value of the optimization.

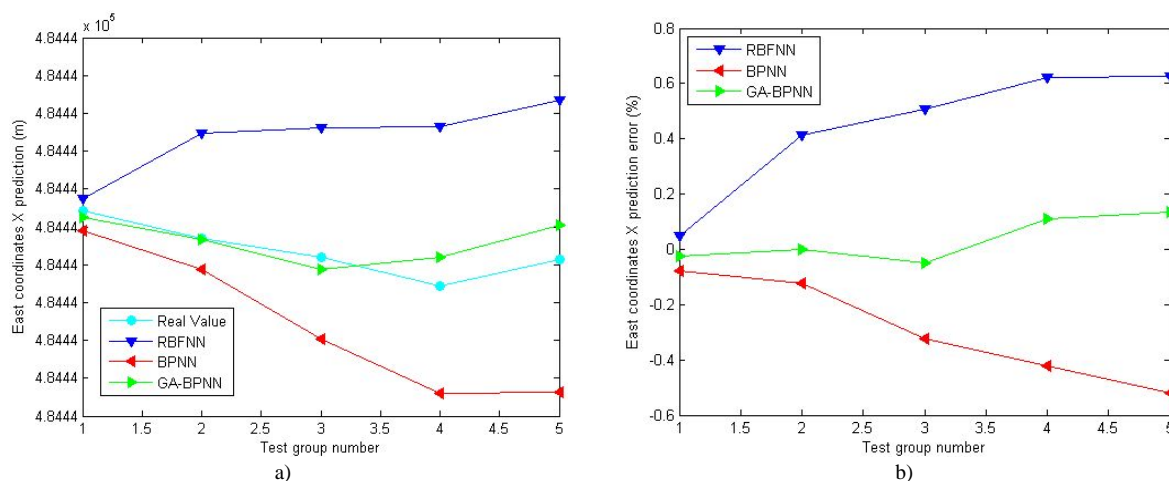


Fig. 8. The forecasting performance: (a) the prediction results of the RBFNN, BPNN, and GA-BPNN, (b) the prediction error of the RBFNN, BPNN and GA-BPNN.

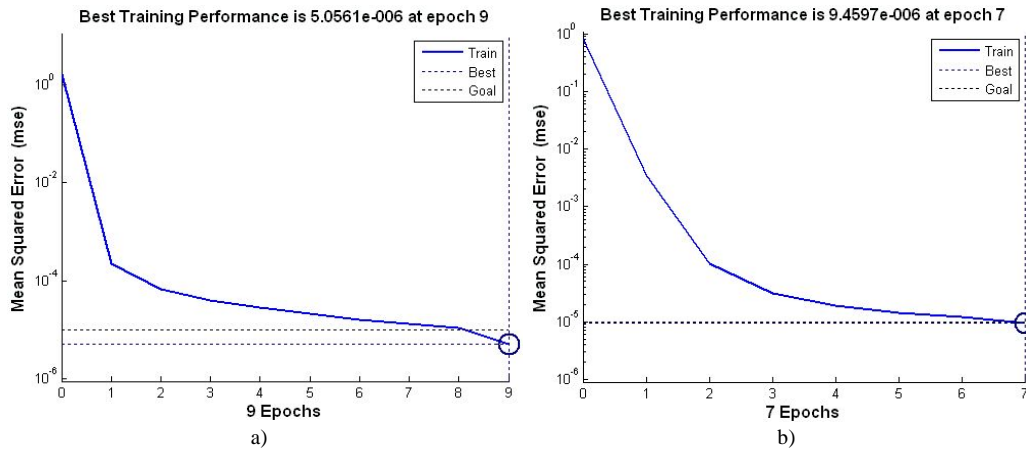


Fig. 9. Comparison of the training performance of two neural networks: (left) BPNN, (right) GA-BPNN.

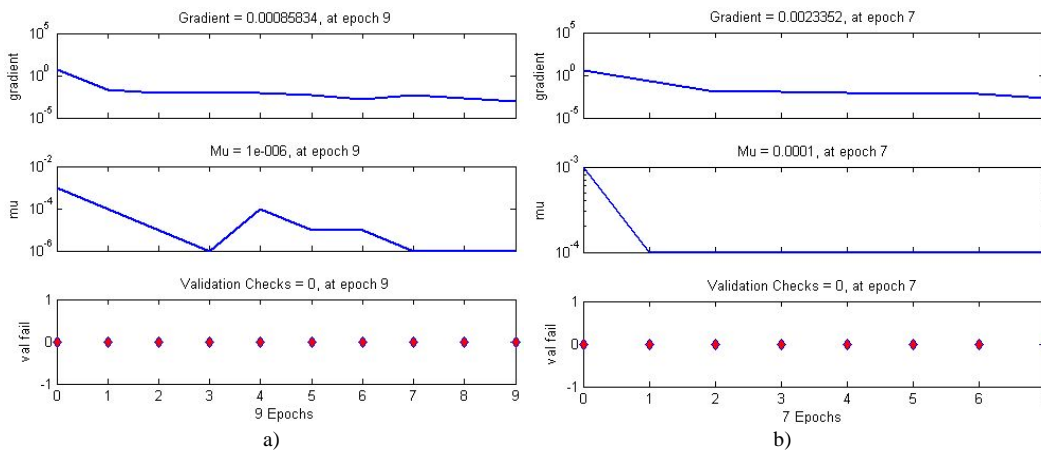


Fig. 10. The training state of two neural networks: (a) BPNN, (b) GA-BPNN.

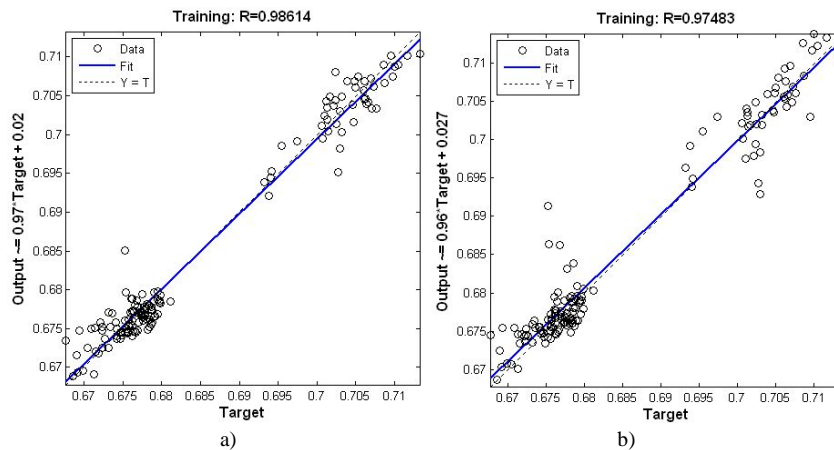


Fig. 11. Regression of two neural networks: (a) BPNN, (b) GA-BPNN.

In addition, Fig. 11 confirms that the regression value of the GA-BPNN is smaller than the BPNN, which suggests that the generalization ability of the GA-BPNN is better than the BPNN. Hence, it can infer that the reason why the gradient index and mutation index of the BPNN is smaller than that of the GA-BPNN is that the BPNN may fall into local minimum in the training while the GA optimizes the BPNN to global minimum. As a result the prediction performance of the BPNN is lower than the GA-BPNN.

Table II shows the comparison between the prediction values using the RBFNN, BPNN and GA-BPNN model. Within the scope of the five prediction test points, the GA-BPNN method prediction values are presenting the best performance. The prediction values for points 1, 2, 3, 4 and 5

using the GA-BPNN method are better than the RBFNN and BPNN methods.

TABLE II. THE PREDICTION VALUE USING RBFNN, BPNN AND GA-BPNN PREDICTION METHOD.

	Point 1	Point 2	Point 3	Point 4	Point 5
<b>Real Value</b>	48443 6.6754	48443 6.6747	48443 6.6742	48443 6.6734	48443 6.6741
<b>RBFNN</b>	48443 6.6928	48443 6.6708	48443 6.6761	48443 6.7243	48443 6.7026
<b>BPNN</b>	48443 6.6749	48443 6.6739	48443 6.6720	48443 6.6706	48443 6.6706
<b>GA-BPNN</b>	48443 6.6753	48443 6.6747	48443 6.6739	48443 6.6742	48443 6.6751

Table III lists the MAE (mean absolute error), MAPE

(mean absolute percentage error) and RMSE (root mean square error) prediction errors. From Table III we can see that the prediction precision of the GA-BPNN is higher than that with RBFNN or just BPNN. For the three patterns, the prediction mean absolute errors of RBFNN and BPNN are 0.0161 and 0.0016, respectively. Contrast with them, the prediction mean absolute error of GA-BPNN is 0.0005. As a result, we can see that the GA-BPNN algorithm has better performance than RBFNN and BPNN.

TABLE III. THE MAE, MAPE AND RMSE USING RBFNN, BPNN AND GA-BPNN PREDICTION METHOD.

	MAE (%)	MAPE (%)	RMSE (%)
<b>RBFNN</b>	0.0161	$3.9100 \times 10^{-6}$	0.0013
<b>BPNN</b>	0.0016	$4.1000 \times 10^{-7}$	0.0012
<b>GA-BPNN</b>	0.0005	$5.0000 \times 10^{-8}$	0.0003

Hence, the GA optimization not only increases the convergence speed of the BPNN in the training process but also the generalization ability. The analysis results show that the proposed GA-BPNN has been proven to be effective in the prediction of the mine slope deformation.

## V. CONCLUSIONS

The monitoring of slope deformation is of great importance for mine safety evaluation. Using intelligent methods to forecast deformation of the mine slope could save manpower and material resources to a great extent. The forecasting approach based on GA-BPNN is therefore presented for accurate prediction of mine slope deformation in this paper. Experimental tests in a real mine slope have been carried out and the analysis results demonstrate that (a) the proposed GA-BPNN is more accurate than the BPNN, (b) the MSE, MAE, MAPE and RMSE of the GA-BPNN are smaller than that of BPNN and RBFNN, and (c) the proposed forecasting approach is feasible and efficient for the forecast of the mine slope deformation. The MAE of the GA-BPNN predictor was 0.0005 and the RMSE was 0.0003. These two criterions fulfill well the actual engineering requirements. Hence, the proposed forecast approach in this work may provide practical utilities for mine slope deformation forecasting.

Future research is planned to further investigate the practical use of the proposed deformation forecasting approach in mining industry. Their industrial application will be explored in the mine safety production.

## REFERENCES

- [1] Y. Jin, F. Xu, "Monitoring and early warning the debris flow and landslides using VHF radar pulse echoes from layering land media", *IEEE Geoscience and Remote Sensing Letters*, vol. 8, pp. 575–579, 2011. [Online]. Available: <http://dx.doi.org/10.1109/LGRS.2010.2093598>
- [2] H. Kratzsch, *Mining Subsidence Engineering*. New York: Springer-Verlag, 1983. [Online]. Available: <http://dx.doi.org/10.1007/978-3-642-81923-0>
- [3] K. Chen, S. Serpico, J. Smith, "Remote sensing of natural disasters", *Proceedings of the IEEE*, vol. 100, pp. 2794–2797, 2012. [Online]. Available: <http://dx.doi.org/10.1109/JPROC.2012.2205835>
- [4] L. Cao, Z. Jiang, "Research on application of artificial neural network in predicting mining subsidence", *Journal of China University of Mining and Technology*, vol. 31, pp. 23–26, 2002.
- [5] T. Ambrozic, G. Turk, "Prediction of subsidence due to underground mining by artificial neural networks", *Computers and Geosciences*, vol. 29, pp. 627–637, 2003. [Online]. Available: [http://dx.doi.org/10.1016/S0098-3004\(03\)00044-X](http://dx.doi.org/10.1016/S0098-3004(03)00044-X)
- [6] J. Deng, "Control problems of Grey system", *Systems and Control Letters*, vol. 5, pp. 288–294, 1982.
- [7] K. Hwang, C. Lo, G. Lee, "A grey synthesis approach to efficient architecture design for temporal difference learning", *IEEE/ASME Transactions on Mechatronics*, vol. 16, pp. 1136–1144, 2011. [Online]. Available: <http://dx.doi.org/10.1109/TMECH.2010.2082558>
- [8] S. Li, H. Zhao, Z. Ru, "Deformation prediction of tunnel surrounding rock mass using CPSO-SVM model", *Journal of central south university*, vol. 19, pp. 3311–3319, 2012.
- [9] C. Kao, C. Loh, "Monitoring of long-term static deformation data of Fei-Tsui arch dam using artificial neural network-based approaches", *Structural Control and Health Monitoring*, vol. 20, pp. 282–303, 2013. [Online]. Available: <http://dx.doi.org/10.1002/stc.492>
- [10] Z. Li, X. Yan, C. Yuan, Z. Peng, L. Li, "Virtual prototype and experimental research gear multi-fault diagnosis using wavelet—autoregressive model and principal component analysis method", *Mechanical Systems and Signal Processing*, vol. 25, pp. 2589–2607, 2011. [Online]. Available: <http://dx.doi.org/10.1016/j.ymssp.2011.02.017>
- [11] Z. Li, X. Yan, Z. Guo, P. Liu, C. Yuan, Z. Peng, "A new intelligent fusion method of multi-dimensional sensors and its application to tribo-system fault diagnosis of marine diesel engines", *Tribology Letters*, vol. 47, pp. 1–15, 2012. [Online]. Available: <http://dx.doi.org/10.1007/s11249-012-9948-1>
- [12] Y. Sun, W. Zeng, Y. Han, "Determination of the influence of processing parameters on the mechanical properties of the Ti-6Al-4V alloy using an artificial neural network", *Computational Materials Science*, vol. 60, pp. 239–244, 2009. [Online]. Available: <http://dx.doi.org/10.1016/j.commatsci.2012.03.047>
- [13] F. Ma, F. Yang, "The prediction of neural network to surface subsidence in mining", *Chinese Journal of Geological Hazard and Control*, vol. 12, pp. 84–87, 1995.
- [14] L. Cao, Z. Jiang, "Research on application of artificial neural network in predicting mining subsidence", *Journal of China University of Mining and Technology*, vol. 31, pp. 23–26, 2002.
- [15] J. Hertz, A. Krogh, R. Palmer, *Introduction to the Theory of Neural Computation*. California: Addison-Wesley, 1991.
- [16] W. Yang, X. Xia, "Prediction of mining subsidence under thin bedrocks and thick unconsolidated layers based on field measurement and artificial neural networks", *Computers and Geosciences*, vol. 52, pp. 199–203, 2013. [Online]. Available: <http://dx.doi.org/10.1016/j.cageo.2012.10.017>
- [17] Z. Li, X. Yan, Z. Guo, Y. Zhang, C. Yuan, Z. Peng, "Condition monitoring and fault diagnosis for marine diesel engines using information fusion techniques", *Elektronika ir Elektrotechnika (Electronics and Electrical Engineering)*, vol. 123, pp. 109–112, 2012.
- [18] N. Kartam and I. Flood, *Artificial Neural Networks for Civil Engineers: Fundamentals and Applications*. New York: ASCE, 1997.
- [19] S. Siu, S. Yang, C. Lee, C. Ho, "Improving the back-propagation algorithm using evolutionary strategy", *IEEE Trans. Circuits and Systems II: Express Briefs*, vol. 54, pp. 171–175, 2007. [Online]. Available: <http://dx.doi.org/10.1109/TCSII.2006.883226>
- [20] E. Brand, J. Premchitt, H. Philipson, "Relationship between rainfall and landslides in HongKong", in *Proc. 4th International Symposium on Landslides*, 1984, pp. 377–384.
- [21] D. Kim, W. Moon, Y. Kim, "Application of TerraSAR-X data for emergent oil-spill monitoring", *IEEE Trans. Geoscience and Remote Sensing*, vol. 48, pp. 852–863, 2010. [Online]. Available: <http://dx.doi.org/10.1109/TGRS.2009.2036253>